

PRECISION CAST Ti-BASED ALLOYS – MICROSTRUCTURE AND MECHANICAL PROPERTIES

M. T. Jovanović, I. Bobić, Z. Mišković, S. Zec

Institute of Nuclear Sciences Vinča, Belgrade, Serbia, tmsj@ptt.rs

Accepted 20.02.2009.

Abstract

The effects of preheat and pouring temperatures as well as annealing temperatures and cooling rates on microstructure and mechanical properties of γ TiAl and Ti-6Al-4V castings have been studied performing X-ray diffraction analysis, light and scanning electron microscopy (SEM), quantitative metallography, hardness and room temperature tensile tests. Annealing of Ti-6Al-4V above and below the β phase transus temperature produces different combinations of strength and elongation, but a compromise may be achieved applying temperature just below the β phase transus. of Ti-6Al-4V alloy. Higher values of tensile strength together with lower ductility than reported in the literature cannot be only ascribed to the presence of α' martensite in the microstructure of Ti-6Al-4V alloy. Ytria coating of graphite crucible must be considered as insufficient in preventing the chemical reaction between aggressive titanium melt and carbon. The processing technology of a “self-supporting” ceramic shell mold was successfully verified during precision casting of both tensile-test samples of Ti-6Al-4V and the prototype of the turbocharger wheel made of γ TiAl. According to experimental results, a processing window for precision casting of the prototype of a turbocharger wheel was established. The results of this paper also show that beside annealing treatment parameters, melting and casting practice together with ceramic mold technology strongly influence the properties Ti-6Al-4V and γ TiAl castings.

Key words: precision casting, “self-supporting” ceramic mold, annealing, phase transformations, strength and elongation, turbocharger wheel

1. Introduction

The most widely used titanium alloy nowadays is Ti-6Al-4V. This alloy possesses an excellent combination of strength, toughness and good corrosion resistance and finds application in aerospace, pressure vessels, aircraft compressor blades and discs, surgical implants *etc.* Aluminum stabilizes the hexagonal close-packed (hcp) α

phase, and vanadium, being body-centered cubic (bcc), stabilizes the β phase. Because of high melting point and excessive reactivity of the melt with crucibles, melting and pouring of titanium alloys have to be performed under vacuum. Due to the high cost of titanium, the use of net-shape or near-net-shape technologies receive an increasing interest considering the large cost saving potential of this technology in manufacturing parts of complex shapes. Precision (investment) casting is by far the most fully developed net-shape technology compared to powder metallurgy, superplastic forming and precision forging. Production of precision castings of titanium alloys was considerably increased during last years due to significant cost savings compared with complicated process of machining.

When Ti-6Al-4V is slowly cooled from the β region, α begins to form below the β transus temperature that is about 980°C [1]. The kinetics of $\beta \rightarrow \alpha$ transformation upon cooling strongly influences properties of this alloy. Contrary to wrought material, however, the possibilities to optimize the properties *via* the microstructural control are limited for cast parts to purely heat treatments. For many alloys mechanical properties of castings are inherently lower than those of wrought alloys. Nevertheless, heat treatment of titanium castings yields mechanical properties comparable, and often superior, to those of wrought products.

Compared with Ti-6Al-4V, which is usually used in the temperature range of 300-550 °C, the γ TiAl aluminides (“ γ alloys”) exhibits a higher oxidation resistance and a lower tendency to hydrogen embrittlement. These alloys with two-phase structure consisting of the major γ phase (ordered TiAl face-centred-tetragonal with $L1_0$ crystal structure) and the minor α_2 phase (ordered Ti_3Al close-packed-hexagonal with DO_{19} structure) were intensively studied within the last decade. They are nearly equal to Ni-based superalloys for turbine blades (Inconel 713C) in specific tensile strength (tensile strength *vs.* density) and specific creep strength (creep strength *vs.* density) over temperatures from 20 to 1000 °C, but are slightly inferior to superalloys in oxidation resistance above 700 °C. However, TiAl alloys do not show appreciable room temperature elongation with a maximum 3% for cast alloys [2-5]. There were some efforts to introduce TiAl castings for the 4th stage compressor turbine blade in jet engines, but further development was called off due to insufficient reliability resulting from low temperature elongation, in spite of other good attributes [3]. In contrast to the tremendously critical requirements for jet engines, it would be far easier to concentrate efforts on technology and application of TiAl aluminides to passenger cars. TiAl aluminides have a high potential to become a new class of structural material to be used mostly in automobile engine construction in the temperature range 500-800 °C.

Advantages to be obtained through the application of TiAl turbocharger rotor to a passenger car are as follows [6]:

- specific power increase which improves vehicle performance,
- improves fuel economy,
- broad engine application range.

The main difficulties in production high quality titanium and titanium alloy castings are: the high melting point, the extremely high reactivity of melt with solids, liquids and gases at high temperatures. For these reasons, traditional casting techniques and materials cannot be used for both melting and molding operations. In addition, melting and pouring have to be performed under vacuum or inert gas. Different crucibles for melting of titanium alloys have been evaluated, *e.g.* graphite and ceramic

crucibles, sometimes inside coated with chemically stable, or slightly reactive compounds with the melt, in order to decrease probability of melt – crucible interaction to occur. The production of investment molds for titanium casting is similar to the production of investment molds for ferrous and superalloys castings [7] except for some very important differences. The major difference is in the investment slurry formulation. Due to a very reactivity of molten titanium a special attention must be paid to the chemical composition of ceramic molds. For these reasons the conventional ceramic molds of silica and zirconia (zirconium silicate), or alumina/silica are not suitable. Molds made of such refractories result in titanium castings having unacceptable surface finish and gross porosity. To avoid these problems, investment molds for titanium castings must be made of special high-stable refractories such as zirconia, thoria and yttria.

The effects of preheat and pouring temperatures as well as annealing temperatures and cooling rates on microstructure and mechanical properties of TiAl and Ti-6Al-4V castings have been studied performing X-ray diffraction analysis, light and scanning electron microscopy (SEM), hardness and room temperature tensile tests.

2. Experimental

2.1 Shell mold preparation, melting and casting procedure

In the present work a “lost wax” procedure was performed to fabricate a “self supporting” ceramic mold [8]. Actually, this procedure represents a modified technology previously successfully applied for production of molds for investment casting of superalloys [9]. The process consists of alternate dipping of a wax pattern (samples for tensile tests) into a colloidal suspension (in which, except for zirconia powder, some quantity of yttria powder was also added) and subsequent pouring with ZrO_2 powder (particle size about 200μ). A “primary coating” (consisting of, at least, three layers) formed by this process must be smooth, chemically stable and with sufficient strength to sustain the pressure of chemically very aggressive melt. In the next step, five to seven layers of the “secondary coating” were produced by pouring mullite (a compound $3Al_2O_3 \cdot 2SiO_2$) with particle size ranging between 200 and 500μ m. “Secondary coating” should enable the strength of the shell mold. The mold was first dried, then de-waxed and fired at $900\text{ }^\circ\text{C}$ for 1h to enable the sufficient strength for handling and the following process of casting. Fig. 1a shows the “self-supporting” ceramic mold after firing of tensile test specimens. The porosity of these molds was between 20 and 25%. The same procedure was performed for turbocharger wheel shell molds (Fig. 1b). The cross-section of a mold showing wax pattern inside the mold together with “primary” and “secondary coatings” is presented in Fig. 1c. The final thickness of a mold was between 5 and 7 mm. The main difference between developed “self supporting” mold and the mold proposed by other manufacturers is that the “self supporting” mold is at least five times lighter offering high chemical stability, high strength and thermal shock resistance at the same time.

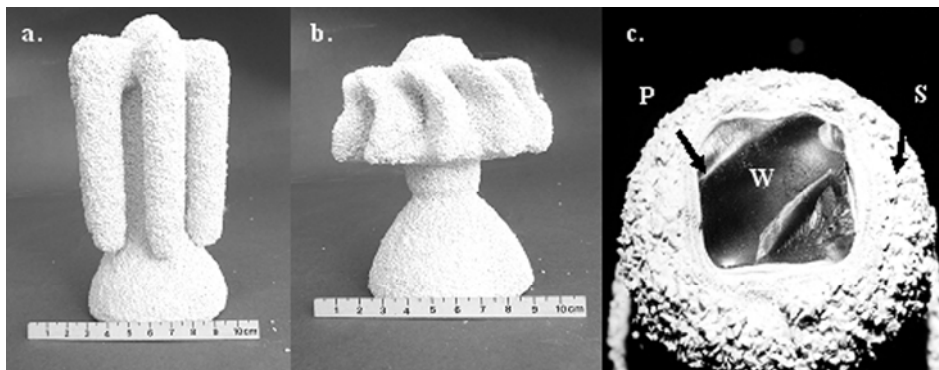


Fig. 1. "Self-supporting" ceramic shell mold. (a) Tensile test specimens; (b) turbocharger wheel; (c) cross-section of ceramic mold P-primary coatings, S-secondary coatings, W-wax

The rods of a commercial Ti-6Al-4V alloy (with the chemical composition 6.4 Al, 3.9 V, 0.35 Fe, less than 0.05 C, the rest was Ti) were melted in a vacuum induction centrifugal furnace "Linn". Graphite crucibles, which inside surface were coated by plasma sprayed yttria, were used for melting. Conditions during melting and casting were as follows: pouring temperature – 1700 °C, preheated temperature of the ceramic shell mold – 600 °C, vacuum during melting and casting – 1Pa, speed of mold rotation – 200 rpm. As soon as the charge was melted, argon was released into the chamber. In order to prevent the possible chemical reaction with crucible, melt was poured into the mold after 2min of holding in the crucible.

To prepare TiAl alloy a "master alloy" in the shape of small ingots (buttons of 50g) was manufactured by vacuum arc-melting of high-purity aluminum (99.5%) and a commercial Ti-6Al-4V alloy. To ensure homogeneous chemical composition buttons were remelted for several times in an argon protective atmosphere. The chemical composition (note: chemical compositions concerning TiAl are given in atomic %) of buttons was: 48Al, 1V, balance Ti. The amount of oxygen was approximately 0.2. The charged stock of "master alloy" was remelted in a "Linn" vacuum centrifugal furnace, whereas the same sort of graphite crucibles and a "self supporting" mold was used as in the case of melting of Ti-6Al-4V alloy. Vacuum pumps were switched off before pouring and the entire system was filled with high purity (99.99%) argon up to 1kPa pressure and the melt was poured into a previously preheated ceramic mold. Conditions during melting and casting were as follows: pouring temperature was varied in the range between 1550 and 1650°C, preheated temperature of ceramic shell mold was varied between 400 and 800°C, speed of mold rotation – 200 rpm, vacuum during processing – 1Pa. Intermetallic compound with the nominal chemical composition Ti-48Al-1V will be referred as TiAl in further text. Approximately the same melting and casting procedure was performed for the processing of turbocharger wheels and specimens for tensile tests. "Self-supporting" ceramic molds demonstrated excellent chemical stability, very good thermal shock resistance coupled with strength to sustain pressure of the melt during solidification. In the same time, it was possible to break molds quite easily without imposing any damage to castings.

2.2 Annealing treatment of Ti-6Al-4V alloy

There are some commonly used annealing treatments for the commercial Ti-6Al-4V alloy. For each of these, the following descriptions are typical of temperatures and times applied, but the actual practice varies with alloy producer and user. According to the literature data [10] a typical procedure involves solutionising at 100 °C above the β transus followed by a cooling and then aging in the $\alpha + \beta$ region. However, other sources [1] suggest solutionising below the β transus which might be followed by aging.

In this study the heat treatment procedure of samples for light microscopy and tensile tests was as follows:

- annealing at 800, 850, 900, 950, 1000, 1050 and 1100 °C for 1h,
- three cooling rates were applied for each annealing temperature, *i.e.*: furnace-cooling, air-cooling and water-quenching.

The heat treatment was performed in the electro-resistance furnace under the protection of flowing argon.

2.3 Characterization of microstructure and mechanical properties

X-ray diffraction analysis with CuK_α irradiation, light microscopy and SEM were used for microstructural characterization. Specimens for these examinations were cut out from the central sprue. Kroll's reagent (a mixture of 10ml HF, 5ml HNO_3 and 85ml H_2O) was used for both alloys as an etchant for light microscopy. The same specimens were used for Vickers hardness tests with applied load of 10 kg. To avoid the possible influence of alpha case (a brittle and relatively deep layer which might be formed on the surface of casting) all hardness measurements were performed in the middle part (core) of the specimens. Screw-type samples for tensile tests produced by investment casting (Fig. 2) were 4mm in diameter and 20mm in gauge length. Uniaxial tensile tests were carried out at room temperature at a strain rate $\dot{\epsilon} = 1.3 \times 10^{-3} \text{ s}^{-1}$.



Fig. 2. Assembly of precision cast samples for tensile tests

3. Results and discussion

3.1 The effect of melting and casting parameters on the quality of castings

As far as Ti-6Al-4V alloy was concerned castings of a good quality (smooth surface, without external porosity and misrun) were obtained. The density of castings was 98% of theoretical density.

However, quite the different situation was encountered in the case of TiAl alloy. The turbine turbocharger wheel casting with 75mm in diameter has a rather complicated configuration consisting of 10 twisted blades with thin (~1 mm) leading edges. Therefore, the precision casting with ceramic investment mold was as a near net-shape processing technique. Some attempts were made with conventional gravity vacuum induction casting, but the quality of castings were unacceptable because they suffered from defects such as misrun, small surface cracks and macroporosity. The most promising technique was found to be centrifugal vacuum casting.

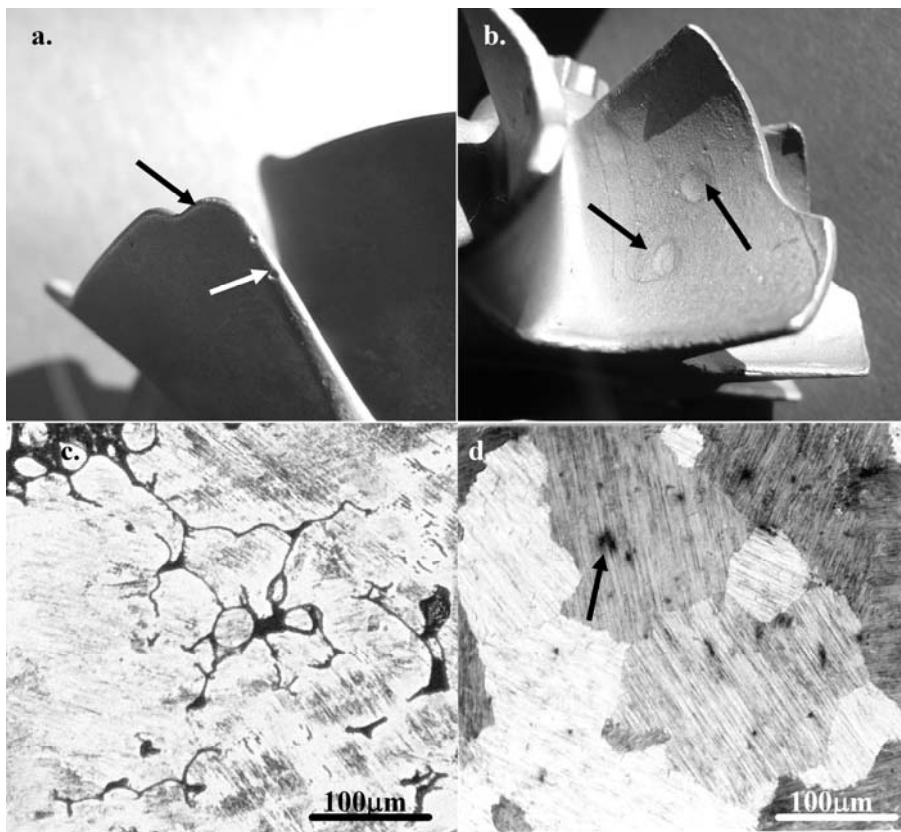


Fig. 3. Macro and micro defects in TiAl alloy caused by inadequate mold preheat or melt pouring temperature. (a) Misrun and small micropores; (b) rough surface and large macropores; (c) interdendritic porosity; (d) micropores.

In addition to mold material, primary interest for the successful casting of TiAl alloy requires careful attention to casting parameters, such as pouring temperature and mold preheat temperature. Mold preheat temperature is one of the most important casting parameters. Higher preheat not only improve fill and feeding, but also reduces thermal gradient and cooling rates. However, higher preheating may lead to severe mold/metal reaction and may increase the propensity for surface-connected porosity. Slower cooling rates may induce coarser grain size and inferior mechanical properties. Therefore, between these parameters a balance must be found in order to achieve properties according to design requirements.

It should be noted that the first castings showed defects such as a misrun and macropores (denoted with arrows in Fig. 3a) when the preheat temperature of molds was below 500 °C. In the case when the preheating was too high (above 800 °C) rough surface and a pronounced macroporosity occurred (Fig. 3b). Pouring temperature above 1600 °C causes a significant extent of interdendritic porosity (Fig. 3c) and microporosity (Fig. 3d).

Applying higher preheat temperature (between 750 and 800 °C) many of these defects were successfully eliminated and a smooth surface together with thin and sharp blade edges were obtained (Fig. 4a,b). The same conditions enabled a good quality of samples for tensile testing.

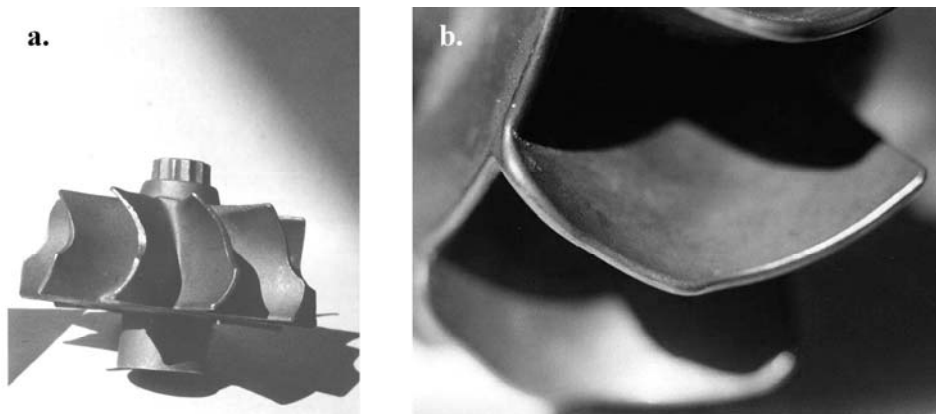


Fig. 4. Correctly cast turbocharger wheel. (a) General look of the turbocharger wheel; (b) detail showing blade edge.

3.2 X-ray diffraction analysis

X-ray diffraction patterns of as-cast Ti-6Al-4V alloy sample and samples annealed at different temperatures then furnace-cooled, air-cooled and water-quenched are shown in Fig. 5(a-c), respectively. Reflections of α and β phase as well as reflections of the face-centered cubic (fcc) phase were detected in diffraction patterns of as-cast and all furnace-cooled samples (Fig. 5a). It should be noted that β reflections are rather weak, suggesting a relatively low volume fraction of the β phase. Diffractograms corresponding to air-cooling (Fig. 5b) are similar to previous regarding the α , β and fcc

phases except that reflections of the α' metastable martensitic phase appear after cooling from β -region above 1000 °C. The broaden α reflections having the fullwidth at half maximum (FWHM) higher than $0.2^\circ 2\theta$ are the evidence for the presence of the supersaturated martensitic phase with hcp structure. Considerable appearance of martensite may be seen in X-ray diffraction patterns of samples water-quenched from 1000, 1050 and 1100 °C (Fig. 5c). In those patterns FWHM of α reflections rise up to $0.8^\circ 2\theta$ due to the martensitic transformation and the formation of hcp diffusionless martensite structure closely related to the hcp structure of the α phase originated from diffusional transformation of a fraction of the β phase. Intensity of α' reflections decreases as the annealing temperature decreases indicating the decrease of the α' fraction. Cooling from the $\alpha+\beta$ region (800 and 900 °C) produces a large fraction of the primary α phase with FWHM less than $0.2^\circ 2\theta$. No traces of the β phase are visible in the patterns of water-quenched samples except from 1050 °C, whereas the fcc phase was observed in all diffractograms.

There is no agreement between authors on the crystal structure of martensite that forms from the β phase. According to some authors [11] two different types of the martensitic phase may form depending on the quenching temperature. These phases are designated as α' , which is fcc or face-centered tetragonal, and the α'' hcp phase. Other authors [12] claim that α'' is orthorhombic, but Malinov *et al.* [13] very recently have suggested that orthorhombic α'' precipitates only upon aging of the supersaturated hcp the α' phase. Since in our paper only a phase having hcp structure upon air-cooling and water-quenching from above 1000°C was detected, the martensitic transformation was designated as $\beta \rightarrow \alpha'$. The presence of some small amount of the β phase in the diffractograms upon quenching from the above the β transus is due to the fact that the martensite finish temperature, M_f , is below 25°C for this alloy [1]. Thus, upon quenching not all β is converted to martensitic α' phase. On the other side, reflections of the fcc phase that may be seen in all diffractograms, including that of as-cast sample, correspond to TiC, TiOC or TiCN according to the fcc lattice parameter of 0.430 nm. It is quite possible that TiC originates from the process of melting – the presence of TiC is the result of the reaction between aggressive Ti-based melt and carbon from crucible, in spite of the fact that inside of crucible was protected by yttria layer.

X-ray diffraction analysis of as-cast TiAl alloy (Fig. 6) proved the existence of α_2 ordered Ti_3Al phase with close-packed-hexagonal lattice ($a = 0.5753\text{nm}$ and $c = 0.4644\text{nm}$) and γ ordered TiAl phase with tetragonal lattice ($a = 0.4016\text{nm}$ and $c = 0.4073\text{nm}$) with c/a ratio of 1.014. This ratio is close to 1.02 which corresponds to the equiatomic TiAl composition, whereas tetragonality increases up to $c/a = 1.03$ with increasing aluminum concentration [5]. A few peaks of retained ordered β (B2) phase, which crystallizes in the CsCl structure, have also been detected. Contrary to castings of Ti-6Al-4V alloy when a peak of TiC and/or TiCN was detected due to reaction of melt and carbon crucible, no presence of carbon in castings was detected in this case.

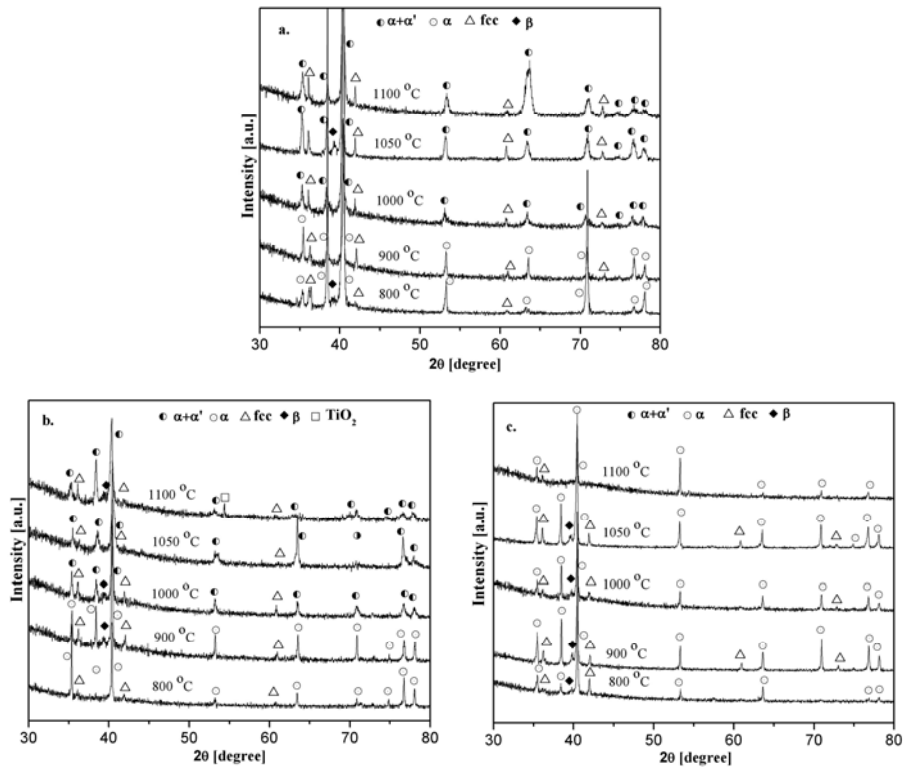


Fig. 5. X-ray diffraction patterns of as-cast Ti-6Al-4V alloy sample and samples annealed at different temperatures then (a) furnace-cooled; (b) air-cooled and (c) water-quenched.

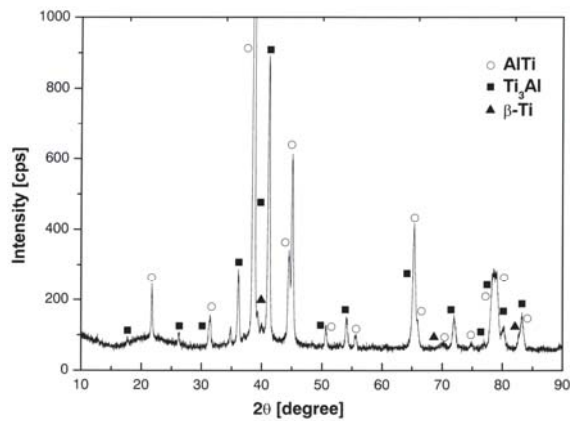


Fig. 6. X-ray diffraction pattern of as-cast TiAl alloy

3.3 Microstructure

Microstructure of as-cast Ti-6Al-4V sample is shown in Fig. 7.

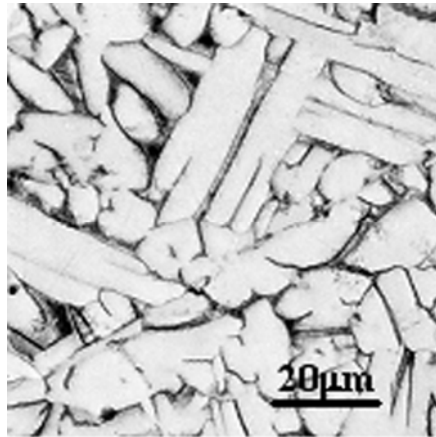


Fig. 7. Microstructure of as-cast Ti-6Al-4V alloy.

As the alloy is slowly cooled from the β region, the α phase begins to appear in the shape of plates below the β transus, with the crystallographic relationship to the β phase in which it forms. The white plates correspond to the α phase, forming a typical Widmanstätten structure, whereas thin dark regions between α plates are the β phase. Some characteristic microstructures after different heat-treatment are shown in Figs. 8-10.

Water-quenching from all annealing temperatures leads to the formation of the α' martensite structure which volume fraction decreases with decreasing temperature. After quenching from 1100 °C α' martensite prevails in the microstructure (Fig. 8a), whereas water-quenching from 950°C produces a mixture of α and β structures with α plates formed inside and at prior β grain boundaries. Some α' martensite is present inside the β phase (Fig. 8b). Similar microstructure is obtained upon water-quenching from 900°C except that the volume fraction of the α phase is higher (Fig. 8c).

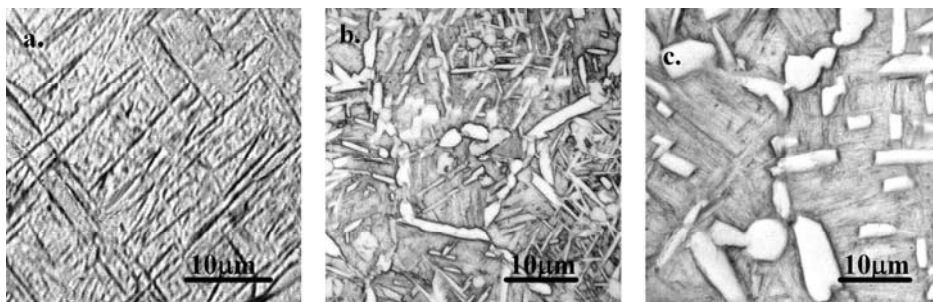


Fig. 8. Light microscope. Microstructure of Ti-6Al-4V alloy upon water-quenching from: (a) 1100 °C; (b) 950 °C; (c) 900 °C

Air-cooling, *i.e.* slower cooling rate leads to the formation of somewhat different type and morphology of microconstituents compared to water-quenching. Upon air-cooling from 1100 °C acicular α_{AC} (transformed β) [14] appear in the β matrix (Fig. 9a). Note that the square or rectangular-like particles are also present in the same microstructure. Morphology of these plates (in the center of some particles very small globule may be seen) is very similar to TiC and TiCN which may be found in some superalloys [15]. This result is also in accordance with the results of X-ray diffraction analysis, supporting the idea that the source for carbides is probably carbon from the graphite crucibles. It is obvious that some β (dark matrix) is transformed to fine acicular α_{AC} upon air-cooling from 1050 °C (Fig. 9b). Primary α plates at boundaries of prior β grains may be also seen. Air-cooling from 950 °C produces structure with higher amount of the α phase at the expense of α_{AC} and β mixture (Fig. 9c).

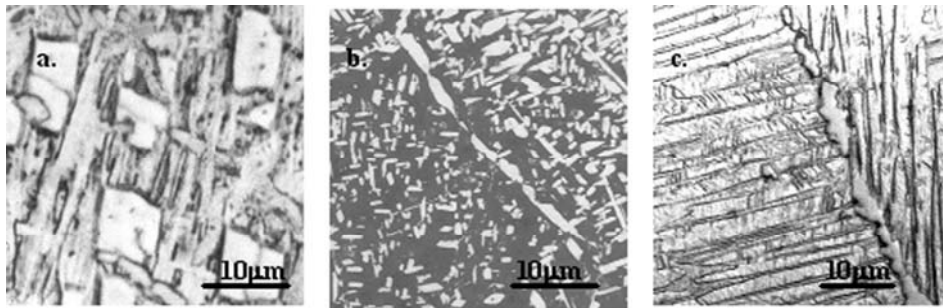


Fig. 9. Light microscope. Microstructure of Ti-6Al-4V alloy upon air-cooling from: (a) 1100 °C; (b) 1050 °C; (c) 950 °C

Plates of the primary α phase with some retained intergranular β are present in samples furnace-cooled from all annealing temperatures (Fig. 10a-c)). Thickness of α plates is higher as annealing temperature is higher, being $\sim 15\mu\text{m}$ at 1100 °C (Fig. 10a), $\sim 10\mu\text{m}$ at 950 °C (Fig. 10b) and $\sim 8\mu\text{m}$ at 800 °C (Fig. 10c). Also, furnace-cooling produces thicker α plates than air-cooling from the same annealing temperature.

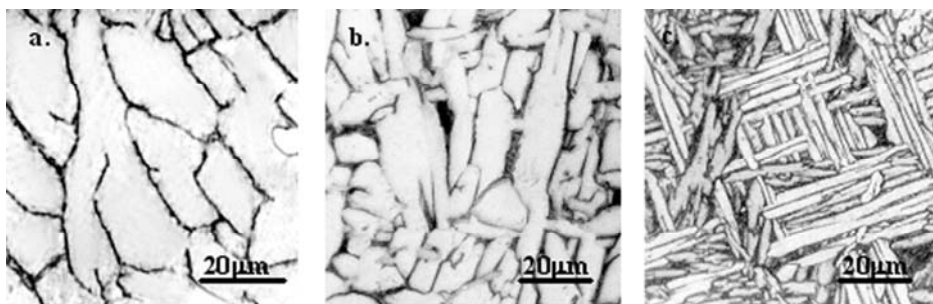


Fig. 10. Light microscope. Microstructure upon furnace-cooling of Ti-6Al-4V alloy from: (a) 1100 °C; (b) 950 °C; (c) 800 °C

When TiAl alloy of composition corresponding to the solid vertical line C is cast from the temperature T_M (around 1600 °C in Fig. 11a) the resulting microstructure consists of grains ranging between 50 and 200 μm . (Fig. 11b).

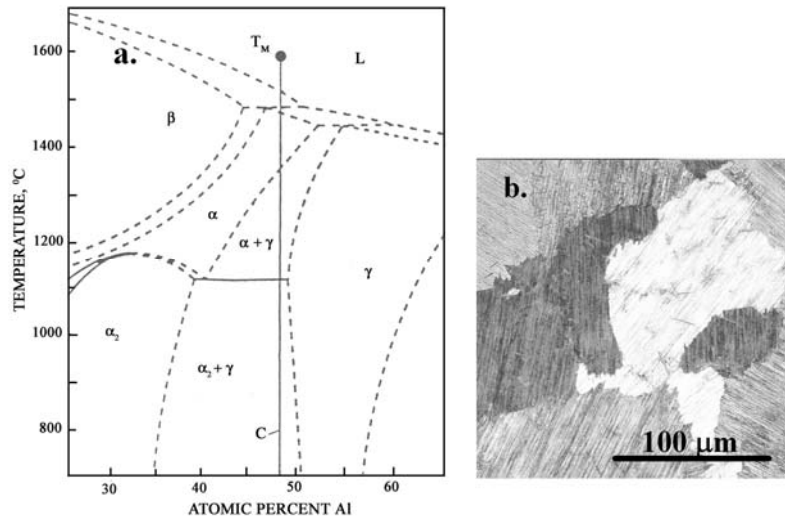


Fig. 11. (a) The central part of the equilibrium Ti-Al phase diagram with C composition line corresponding to Ti-48Al alloy [16]. (b) Light microscope. Grains of different size in the as-cast microstructure of TiAl alloy

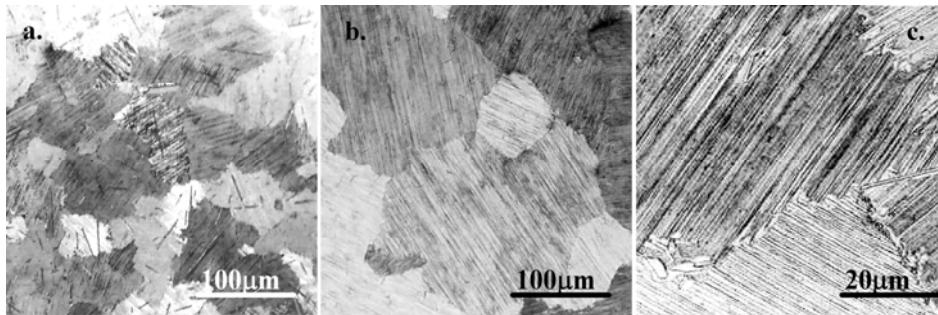


Fig. 12. Light microscope. As-cast microstructure of Ti-48Al-IV alloy. (a) Mold preheated at 500 °C; (b) mold preheated at 800 °C; (c) Higher magnification of specimen shown in b illustrating lamellar structure. Light contrast corresponds to the β phase (B2)

In addition to cooling rate the as-cast microstructure of TiAl alloy depends on the chemical composition. Some literature data show that grains are becoming smaller with decreasing aluminum content and with small additions of vanadium, manganese and chromium [17,18]. However, in the case of this work the cooling rate during solidification was a predominant factor influencing the grain size. Higher cooling rate (mold was preheated at 500 °C) yielded grains between 100 and 300 μm in size (Fig.

12a), whereas lower cooling rate (mold temperature was around 800 °C) produced rather coarse (between 300 and 600 μm) grains (Fig. 12b). Higher magnification clearly reveals that coarse grains possess the fully lamellar microstructure where the lamellae are mostly γ intermixed with dark lamellae of the α_2 phase (Fig. 12c). Individual rod-like particles and particles at grain boundaries (having light contrast) of the β (B2) phase may be also seen in the same micrograph. A similar morphology of this phase was reported in ingots of Ti-47Al-4(Cr,Nb,Mo,B) [19].

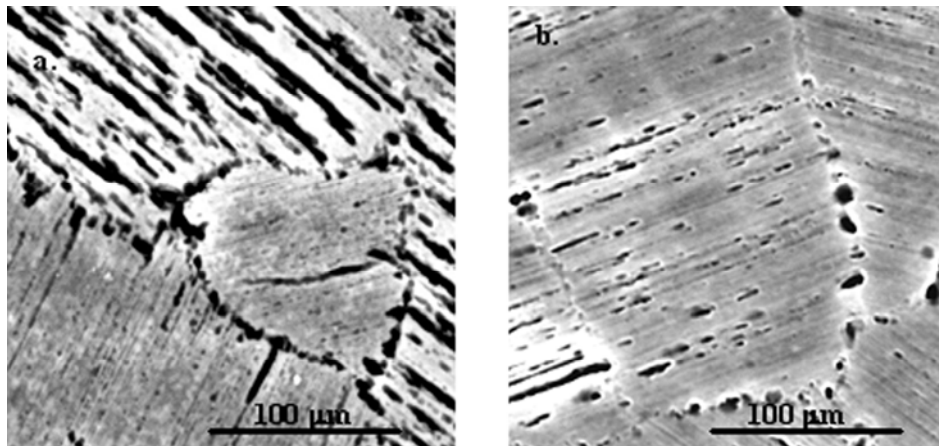


Fig. 13. SEM. Secondary electrons. The effect of preheat mold temperature (cooling rate) on α_2/γ lamellar spacing of TiAl alloy. (a) Slower cooling rate; (b) higher cooling rate

Although a number of experiments was performed applying variations of pouring temperature and preheating temperature of the ceramic shell, the appearance of some porosity could not be avoided. To preserve this lamellar structure that might be lost during HIP [20], no experiments with HIP have been performed in order to eliminate microporosity. In general, lamellar structure could result in low ductility (even less than 1%) [21], but with regard to creep properties a fully lamellar structure is desirable [22, 23]. Lamellar spacing was found to depend on cooling rate (Fig. 13a,b), *i.e.* in coarse grains (slower cooling rate, Fig. 13a) this spacing was somewhat larger than in smaller grains (higher cooling rate, Fig. 13b). This is in accordance with the results of Kim [24] who reported the effect of cooling rate on α_2/γ spacing.

3.4 Mechanical properties

Mechanical properties of Ti-6Al-4V alloy as a function of annealing temperatures and cooling rates are illustrated in Table 1.

In general, tensile strength increases with increase in annealing temperature being highest upon water-quenching, whereas upon furnace-cooling the lowest strength values were registered. A saturation of strength was reached after 1050 °C and the plateau was formed between 1050 and 1100 °C. On the other hand, elongation decreases with increasing both annealing temperature and cooling rate. In addition, values of

strength and ductility of as-cast samples are lower than those after heat treatment. The highest values of strength, although accompanied with the lowest elongation, are obtained when the martensitic α' phase is produced upon water-quenching irrespective of annealing temperature, indicating that caution should be exercised if applying this annealing treatment. According to the results of X-ray diffraction analysis, light microscopy and tensile tests, a compromise between adequate values of strength and elongation may be achieved with the annealing temperature just below the β transus, *i.e.* between 900 and 950 °C, and applying air-cooling as a moderate cooling rate. Some improvement in elongation could be achieved with the finer thickness of the primary α plates.

Table 1. The effect of different annealing temperatures and cooling rates on mechanical properties of Ti-6Al-4V alloy

Temp., °C	Water-quenched		Air-cooled		Furnace-cooled	
	Tensile strength, MPa	Elongation, %	Tensile strength, MPa	Elongation, %	Tensile strength, MPa	Elongation, %
1100	1385	1.5	1350	1.8	1230	2.6
1050	1390	1.5	1350	1.8	1290	2.5
950	1310	1.8	1290	2.4	1230	2.9
900	1250	2.0	1190	2.8	1150	3.5
800	1200	2.5	1165	3.0	1120	4.0

The data on values on mechanical properties of heat-treated Ti-6Al-4V alloy castings are rather limited. Comparing the results of this paper with the literature data (tensile strength: 980-1150MPa; elongation: 8-10%, although the parameters of heat treatment were not specified) [25-27] it is obvious that the values of tensile strength from Table 1 are higher, but elongation is rather lower. To account for these values, although the effect of α' martensite on tensile strength and elongation cannot be neglected, the process of melting of Ti-6Al-4V should be analyzed in view of some important details. Namely, although the graphite crucible was coated with yttria coating it is quite possible that during melting this coating was damaged and some amount of carbon diffused into the melt forming carbides with titanium and vanadium. The presence of TiC was documented by X-ray diffraction analysis in as-cast and all annealed samples. This type of carbide was also identified by light microscopy (Fig. 9a). Considering that even a small amount of carbon significantly increases strength (*eg.* increase of carbon from 0.1 to 0.2 wt.% raises tensile strength between 60 and 80 MPa and deteriorates ductility for about 5% [28]) it is quite possible that the higher level of strength and unexpectedly low values of elongation are the result of increase of carbon content in the alloy due to its absorption during melting. From this point of view it is obvious that coating protection of graphite crucible by yttria proved to be ineffective. Evidently, according to the results of this paper the utmost care must be paid to the protective coating of graphite crucibles, but the quality of the crucible itself (density of graphite, type of binder) must not be neglected. Also, parameters of melting practice such as time of holding the melt in the crucible, intensity of induction field, interrelation between the height of charge and the height of induction coil affect the quality of

castings. For melting of high quality titanium alloys, apart from expensive skull melting with the cold crucible which enables contamination-free castings, a very recent literature report suggests the application of less expensive standard casting practice, but with ceramic crucibles made of yttria and calcia [29].

Room temperature mechanical properties of TiAl-based alloys (with a chemical composition similar to alloy of this work) are compared in Table 2.

Table 2. Room Temperature Mechanical Properties of Some TiAl-Based Alloys

Alloy, at. %	Strength, MPa		Elongation, %	Hardness, HV ₁₀	Ref.
	Yield Strength	Ultimate Tensile Strength			
Ti-48Al-1V* (100÷200µm)	430	500	1.2	360	This paper
Ti-48Al-1V* (300÷500µm)	400	475	1.8	330	This paper
Ti-48Al*	390	483	0.-2.1	250	[3]
Ti-48Al-1V	400	507	2.3	-	[3]
Ti-44Al-1V	754	-	0.6	-	[30]
Ti-48Al(1-3)V	520	-	1.5-3.5	-	[3]
Ti-48Al-2Nb-2Mn (as-cast+HIPed)	392	460	0.9	-	[31]
Ti-47Al-5Nb*	480	510	0.5	-	[32]
Ti-47Al-2Cr-2Nb*	560	659	1.6	300	[33]

*As-cast

Concerning the results of mechanical properties the results of this paper represent the average value of four tests. The effect of smaller grain size on mechanical properties on TiAl-based alloys is evident, *i.e.* higher strength and hardness, but lower elongation showed samples solidified under higher cooling rate. Although in most alloys the previous “thermal history“ was not specified, it is obvious that the results of this paper quite well agree with the literature data. Considering the results of mechanical testing presented in this paper one should be cautious since these values refer not to the turbocharger wheel itself, but to tensile specimens solidified under the conditions intended to be similar during solidification of casting with different geometry.

Based on inspection of casting, microstructural analysis and mechanical properties, a processing window for precision casting of a prototype of the turbocharger wheel made of TiAl alloy may be established, *i.e.* pouring temperature: between 1580 and 1600 °C; shell mold preheating temperature: between 750 and 800 °C; speed of mold rotation: 200 rpm; vacuum during melting: 1Pa. Although with mold preheat temperature at 500 °C smaller grains and higher strength were achieved, higher preheat temperature was chosen due to better quality of surface castings. Applying these parameters, the prototype of the TiAl turbocharger wheel having yield strength – 400MPa, ultimate tensile strength – 475MPa, elongation – 1.8%, hardness – 330HV and grain size – between 300 and 500µm was produced.

4. Conclusions

The effects of preheat and pouring temperatures as well as annealing temperatures and cooling rates on microstructure and mechanical properties of γ TiAl alloy (with the nominal chemical composition Ti-48Al-1V) and Ti-6Al-4V castings have been studied performing X-ray diffraction analysis, light and scanning electron microscopy (SEM), hardness and room temperature tensile tests.

Annealing of Ti-6Al-4V above and below the β phase transus temperature produces different combinations of strength and elongation, but a compromise may be achieved applying temperature just below the β phase transus. Higher values of tensile strength together with lower ductility than reported in the literature cannot be only ascribed to the presence of α' martensite in the microstructure. Yttria coating of graphite crucible must be considered as insufficient in preventing the chemical reaction between aggressive titanium melt and carbon.

The processing technology of a "self-supporting" ceramic shell molds was successfully verified during investment casting of both tensile-test samples of Ti-6Al-4V and the prototype of the turbocharger wheel made of γ TiAl alloy. "Self-supporting" ceramic shell molds demonstrated excellent chemical stability together with strength to sustain pressure during solidification.

According to experimental results, a processing window for precision casting of the prototype of a turbocharger wheel was established. The results of this paper also show that beside annealing treatment parameters, melting and casting practice together with ceramic mold technology strongly influence the properties Ti-6Al-4V and γ TiAl alloy castings.

Acknowledgement

The work was financially supported by the Ministry of Science and Technological Development of the Republic of Serbia through the Projects Nos. 1966 and 142027.

5. References

- [1] C.R. Brooks, "Heat Treatment, Structure and Properties of Non Ferrous alloys", Metals Park, OH: ASM International; 1982.
- [2] Y.W. Kim, J. Metals 46 (1994) 30-39.
- [3] Y.W. Kim, *ibid.* 41 (1989) 24-30.
- [4] R.V. Ramanujan, *Int. Mat. Rev.* 45 (2000) 217-242.
- [5] H. Klemens, H. Kestler, *Adv. Eng. Mat.* 2 (2000) 551-570.
- [6] Y. Nishiyama, T. Miyashita, S. Isobe, T. Noda, In: *High Temperature Aluminides and Intermetallics*, Eds.: Wang S.H., Liu C.T., Pope D.P., Stiegler J.O., Indianapolis, TMS 1990, p. 557
- [7] Milan T. Jovanović, Borislav Lukić, Zoran Misković, Ilija Bobić, Ivana Cvijović, Biljana Dimčić, *Metalurgija-Journal of Metallurgy* 13 (2007) 91-106.
- [8] I. Bobić, S.Tadić, M.T Jovanović, I. Đurić, M. Pantović, SRPS Patent 2003; No. 449/03 (patent pending).

- [9] Z. Mišković, M.T. Jovanović, M. Gligić, B. Lukić, *Vacuum* 43 (1992) 709-711.
- [10] RV Noort., *J. Mat. Sci.* 22 (1987) 3801-3811.
- [11] C. Hammond, J. Nutting, *Met. Sci.* 10 (1977) 474-489.
- [12] R. Boyer, G. Welsh, E.W. Collings, editors. "Handbook Titanium Alloys". Materials Park, OH: ASM International; 1994.
- [13] S. Malinov, W. Sha, Z. Guo, C.C. Tang, A.E. Long, *Mat. Charact.* 48 (2001) 279-295.
- [14] *Metals Handbook. Metallography and microstructures.* 9th ed. Materials Park, OH; ASM International; 1986.
- [15] M.T. Jovanović, Z. Mišković, B. Lukić, *Mat. Charact.* 40 (1998) 261-298.
- [16] C. McCullough, J.J. Valencia, H. Mateos, C.G. Levi, R. Mehrabian, K.A. Rhyne, *Scripta Met.* 22 (1988) 1131-1136.
- [17] T. Tetsui, Y. Miura, *Mitsubishi Heavy Industries Technical Review*, 39 (2002) 592-597.
- [18] H. Clemens, A. Lorich, N. Eberhardt, W. Glatz, W. Knabl, H. Kestler, *Metallkde* 90 (1999) 569-580.
- [19] H. Clemens, F. Jeglitsch, *Prakt. Metall.* 37 (2000) 194-217.
- [20] T. Tetsui, *Mat. Sci. Eng.* A329-331 (2002) 582-588.
- [21] Y.W. Kim, D.M. Dimiduk, In: *Structural Intermetallics 1997*, Eds.: Nathal M.V., Darolia R., Liu C.T., Martin P.L., Miracle, D.B., Wagner, R., Yamaguchi, M., Warrendale, The Minerals, Metals and Materials Society 1997, p.531.
- [22] P.A. McQuay, V.K. Sikka, *Casting*, In: *Intermetallic Compounds, vol.3, Principles and practice*, Eds.: Westbrook, J.H., Fleischer, R.L., New York, John Willey and Sons 2000, p.592.
- [23] D.M. Dimiduk, D.B. Miracle, Y.W. Kim, M.G. Mendiratta, *ISIJ Int.* 31 (1991) 1223-1234.
- [24] Y.W. Kim, *Mat. Sci. Eng.* A192-193 (1995) 519-533.
- [25] ASTM Standard F 1108-02. Standard specification for titanium-6aluminum-4vanadium surgical implants. (UNS 54406).
- [26] D.L. Ruckle, P.P. Millan, U.S. Patent 1986; No. 4.631.092.
- [27] D. Eylon, W.J. Barice, F.H. Froes, *SAMPE* 17 (1985) 585-595.
- [28] R.I. Jaffee, Titanium-base alloys, In: *Progress in metal physics*, Eds.: Chalmers, B., King, R., New York, Pergamon Press 7 1958, p. 646.
- [29] J. Barbosa, C.S. Ribeiro and C. Monteiro, *Intermetallics* 15 (2007) 945-955.
- [30] H.A. Lipsitt, In: *Mat. Res. Soc. Symp. Proc.* 39, Pittsburgh, MRS 1985, p.351.
- [31] J.P. Kuang, R.A. Harding, J. Campbell, *Mat. Sci. Eng.* A329-331 (2002) 31-37.
- [32] R. Yang, Y.Y. Cui, L.M. Dong, Q. Jia, *J. Mat. Proc. Techn.* 135 (2003) 179-188.
- [33] W. Shouren, G. Peiquan, Y. Liying, *ibid.* 204 (2008) 492-497